Title

Nanometer-Scale Force Profiles of Short Single- and Double-Stranded DNA Molecules on a Gold Surface Measured Using a Surface Forces Apparatus

Journal

Langmuir, 37(45)

ISSN

0743-7463

Authors

Kang, Di
Yu, Jing
Xia, Fan
et al.

Publication Date

2021-11-16

DOI

10.1021/acs.langmuir.1c01966

Peer reviewed

Published in final edited form as:

Langmuir. 2021 November 16; 37(45): 13346–13352. doi:10.1021/acs.langmuir.1c01966.

Nanometer-Scale Force Profiles of Short Single- and Double-Stranded DNA Molecules on a Gold Surface Measured Using a Surface Forces Apparatus

Di Kang,
Department of Chemistry and Biochemistry, University of California, Santa Barbara, Santa Barbara, California 93106, United States;

Jing Yu,
School of Materials Science and Engineering, Nanyang Technological University, 639798, Singapore;

Fan Xia,
Engineering Research Center of Nano-Geomaterials of Ministry of Education, Faculty of Materials Science and Chemistry, China University of Geosciences, Wuhan 430074, China;

Jun Huang,
Department of Chemical and Materials Engineering, University of Alberta, Edmonton, AB T6G 2V4, Canada;

Hongbo Zeng,
Department of Chemical and Materials Engineering, University of Alberta, Edmonton, AB T6G 2V4, Canada;

Matthew Tirrell,
Pritzker School of Molecular Engineering, University of Chicago, Chicago, Illinois 60637, United States; Center for Molecular Engineering, Argonne National Laboratory, Argonne, Illinois 60439, United States;

Jacob Israelachvili,
Department of Chemical Engineering, University of California, Santa Barbara, Santa Barbara, California 93106, United States;

Kevin W. Plaxco

Corresponding Authors: Kevin W. Plaxco – Department of Chemistry and Biochemistry, University of California, Santa Barbara, Santa Barbara, California 93106, United States; Interdepartmental Program in Biomolecular Science and Engineering, University of California, Santa Barbara, Santa Barbara, California 93106, United State, kwp@chem.ucsb.edu, **Hongbo Zeng** – Department of Chemical and Materials Engineering, University of Alberta, Edmonton, AB T6G 2V4, Canada; hongbo.zeng@ualberta.ca.

Author Contributions

D.K. and J.Y. contributed equally to this paper.

Supporting Information

The Supporting Information is available free of charge at https://pubs.acs.org/doi/10.1021/acs.langmuir.1c01966.

Force–distance profiles for a bare mica surface pressed against a hydroxyl-terminated SAM surface and a SAM-coated surface modified with a 25-base DNA (PDF)

Complete contact information is available at: https://pubs.acs.org/10.1021/acs.langmuir.1c01966

The authors declare no competing financial interest.

Department of Chemistry and Biochemistry, University of California, Santa Barbara, Santa Barbara, California 93106, United States; Interdepartmental Program in Biomolecular Science and Engineering, University of California, Santa Barbara, Santa Barbara, California 93106, United States;

Abstract

Using a surface forces apparatus (SFA), we have studied the nanomechanical behavior of short single-stranded and partially and fully double-stranded DNA molecules attached via one end to a self-assembled monolayer on a gold surface. Our results confirm the previously proposed "mushroom-like" polymer structure for surface-attached, single-stranded DNA at low packing density and a "brush-like" structure for the same construct at higher density. At low density we observe a transition to "rigid rod" behavior upon addition of DNA complementary to the surface-attached single strand as the fraction of molecules that are double-stranded increases, with a concomitant increase in the SFA-observed thickness of the monolayer and the characteristic length of the observed repulsive forces. At higher densities, in contrast, this transition is effectively eliminated, presumably because the single-stranded state is already extended in its "brush" state. Taken together, these studies offer insights into the structure and physics of surface-attached short DNAs, providing new guidance for the rational design of DNA-modified functional surfaces.

Graphical Abstract

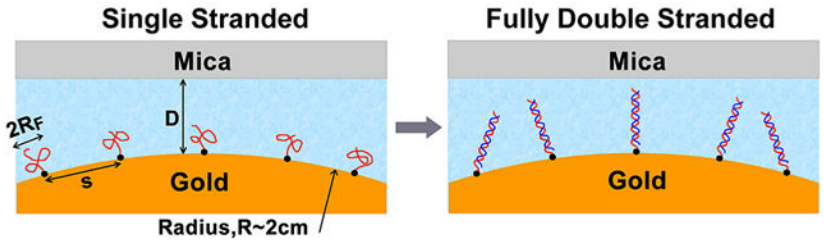

INTRODUCTION

Surface-grafted oligonucleotides play important roles in many biotechnologies. Next-generation DNA sequencing, expression screening, synthetic biology, and many biosensor architectures, for example, employ surface-bound DNAs or RNAs to perform the recognition of not only specific oligonucleotides but also proteins and small molecules.[1–6] Despite the growing technological importance of oligonucleotide-modified surfaces, however, our understanding of the physics of such surface-attached biomolecules remains in its infancy.[7–11] For example, the large majority of previous studies in this field focused on relatively long oligonucleotides, demonstrating that these follow the physics expected for surface-attached polyelectrolytes.[12–15] In contrast, most of the technologies employing surface-bound oligonucleotides use molecules quite short relative to the persistence length of the double helix[16] and that, in support of their function, often adopt complex secondary structures.[13] Despite this, few prior studies have directly addressed the physics of such short biopolymers tethered to surfaces.[11,13,17–23]

The lack of data regarding the physics of short, surface-bound oligonucleotides is not without consequences. To illustrate this, we point the reader to electrochemical DNA (E-DNA) and electrochemical aptamer-based (EAB) sensors, the signaling of which is a sensitive function of the density at which their short oligonucleotide recognition "probes" are packed onto the surface of the interrogating electrode.[24,25] The gain (the relative signal change seen at saturating target) of linear probe E-DNA sensors, for example, rises strongly with increasing probe density at low densities before leveling off at high densities, presumably due to interactions between adjacent oligonucleotides that reduce the ability of an attached redox reporter to approach the surface and generate a current. To date, however, this factor can only be optimized empirically due to our limited understanding of the conformations sampled by surface-bound DNAs and how these vary with the density at which the DNA is packed onto the surface. Motivated by the argument that improved understanding of the properties and interaction mechanisms of surface-attached oligonucleotides could help to enhance the performance of technologies dependent on biomolecules site-specifically attached to a surface, we have used a surface forces apparatus (SFA) to measure the nanomechanical properties and molecular interaction forces of short single- and double-stranded DNA molecules attached via one end to a self-assembled monolayer (SAM) on a gold surface (Figure 1). The resulting force–distance profiles can be correlated to the structure and force-induced conformational changes of the surface-bound biomolecules.

The SFA allows direct measurement of the force between two macroscopically curved surfaces as a function of their separation with subnanometer resolution, providing quantitative insights into the thickness and mechanical properties of a molecular layer grafted on one or both. Taking advantage of this technique, we have measured the effects of packing (grafting) density on the interfacial properties and interactions of short, single-stranded, partially double-stranded, and fully double-stranded DNA molecules attached to a gold surface via a six-carbon alkanethiol attached to the 5′ terminus of one strand. The surface is then backfilled with 6-mercapto-1-hexanol to form a hydroxyl-terminated surface.

RESULTS AND DISCUSSION

To study the behavior of surface-attached DNA molecules, we started with the simplest example: DNA attached to the surface by one terminus and at relatively low packing density (i.e., relatively few molecules per unit area) and relatively high ionic strength (Figure 2a), such that interactions between adjacent molecules are minimized. Specifically, we measured the interaction forces between a bare mica surface and a SAM-coated gold surface modified with a sparse submonolayer of a 25-base, single-stranded DNA immersed in phosphate buffer containing 0.6 M NaCl (Figure 2b, black symbols). At this ionic strength, electrostatic interactions are largely screened (the Debye length, $1/\kappa = 0.4$ nm, is approximately equal to the length of one base), leaving the interactions of the system dominated by entropic and steric forces between the DNA and the approaching surface. (Of note, only weak adhesion forces are detected when separating a bare mica surface and a hydroxyl-terminated SAM-modified gold surface under these conditions,[26] thus simplifying our analysis; see Figure S1.)

The repulsion between bare mica and our single-stranded-DNA-modified surface first becomes apparent when the two approach to within ~10 nm, after which it increases exponentially (i.e., the force–distance profiles are linear on a semilog plot). When the two surfaces approach to within ~2 nm, the force rises to 10 mN/m, at which a so-called "hard-wall" distance is reached for approach of the surfaces. That is, further increases in the applied load do not alter the distance after this point. Of note, the distance at which we first observe repulsion is longer than the ~8 nm contour length of a 25-base, single-stranded DNA.[27] Similar long-range repulsion has previously been reported for other DNA-modified surfaces[20,28] and has been attributed to long-range hydration forces by Hagen and Chakraborty, who support this with theoretical analyses performed over a broad range of surface grafting densities.[10]

The mechanical properties of the 25-base, single-stranded submonolayer change significantly when the DNA is hybridized with its full-length complement to form a double helix (Figure 2a). To see this, we titrated the surface-attached, single-stranded DNA against 50 aM, 500 aM, 1 pM, and 50 pM of its full-length complement, monitoring the force–distance profile after equilibration (Figure 2b and Figure S2). Doing so, we find that the repulsive force between two surfaces measured at a fixed separation distance increases monotonically with increasing complement concentration, presumably due to the enhanced steric and electrostatic repulsion of the increasing fraction of the double helix. For example, while the repulsion for the single-strand surface starts at ~9 nm, this extends to ~12 nm upon the addition of 50 aM complement and remains at this value up to the highest compliment concentrations we have employed (at which hybridization is expected to be effectively complete). The hard-wall distance likewise increases upon hybridization, reaching 6 nm, which is some 3 times greater than the 2 nm hard-wall distance seen for the single-stranded submonolayer case under the same compression force (Figure 2b).

The force profiles of a 25-base construct that is partially double helical and partially single stranded differ from those of the 25-base pair full double helix. Specifically, when we titrated the surface-attached single-stranded DNA with sequentially increasing concentrations of a 13-base complement, producing a 13 base-pair double helix flanked on either side by six-base single-stranded regions (Figure 3a and Figure S3), the first repulsion is seen at ~10 nm (Figure 3b), a shorter distance than the ~12 nm seen for the completely double-helical construct (Figure 2). The final hard wall of the partially double-helical construct is likewise some 2 nm shorter than the 6 nm seen for the completely double-helical construct. The differing force profiles of the completely and partially double-helical constructs (both of which are of similar length when fully extended) presumably reflect their differing flexibilities. For example, with a length of about 8 nm a 25-base-pair double helix is much shorter than its ~50 nm persistence length,[29] suggesting that while these constructs are free to rotate and tilt (due to the flexible phosphodiester used to anchor the 5′ end of one strand to the monolayer), the completely double-helical construct acts as if it is rigid. The partially double-helical construct, in contrast, is composed of a rigid 13-base-pair double-stranded element flanked by flexible, six-base single-stranded elements (Figure 3a). These flexible ends lead to a less rigid submonolayer with a smaller range of repulsion and a shorter hard-wall distance than for the completely double-helical construct.

The minimum concentrations of complementary strand at which we see hybridization-driven changes in repulsion are higher than we expect given calculated binding free energies. For example, when calculated by using the M-fold software,[30] the estimated binding free energy of our 13-base complementary DNA sequences is −75 kJ/mol under the conditions we employ, yielding an estimated equilibrium dissociation constant, K_D, of ~10^{-13} M. Our surface force measurements, however, do not exhibit any significant shift in the force profiles until the concentration of complement reaches an order of magnitude higher than the calculated dissociation constant (Figure 3b). Likewise, for the 25-base complement the estimated equilibrium dissociation constant is ~10^{-28} M, orders of magnitude below the concentration at which we first see an increase in repulsion. We suspect that these deviations are due to the limited number of molecules present in the 15 μL volume over our surfaces; the limited number of complement molecules present in this volume prevents hybridization from reaching saturation until concentrations quite far above the dissociation constant are reached.[31]

The interactions and the resultant mechanical properties of surface-attached DNA molecules are also strong functions of the density with which they are packed on the surface. To explore this, we prepared surfaces modified upon with the same 25-base single-stranded DNA using conditions that previous electrochemical[24] and surface plasmon resonance measurements[18,32] indicate lead the density of either ~0.01 or ~0.1 chain/nm^2. The resulting force profiles produce two distinct behaviors (Figure 4a). The force profile we observe at lower density is linear on a semilog plot, with notable repulsion beginning at ~10 nm that increases to hard-wall repulsion at ~2 nm (Figure 4a; black data points). In contrast, force profiles collected at the higher density exhibit longer-range repulsion (~12 nm, about the contour length of a 25-base single-stranded DNA[33,34]), a steeper slope on the semilog plot, and a shift in the hard-wall cutoff from ~2 to ~6 nm (Figure 4a; red data points). The density dependencies of these force profiles presumably arise due to the well-known “mushroom-to-brush” transition of unstructured, surface-tethered polymers.[35] At low density, neighboring chains do not interact, and each single-stranded chain forms a distorted random coil that is perturbed by the surface into a mushroom-shaped ensemble (Figure 4b). At high density interactions between neighboring chains cause each to extend further from the surface, resulting in a brush-like ensemble (Figure 4c).

To quantitatively explore the mushroom-to-brush transition, we modeled the force profiles obtained at lower and higher densities using polymer-scaling theory. The free energy of a surface-attached single-stranded DNA in the mushroom configuration confined between two planar surfaces can be approximated by an exponential repulsive potential:[35]

$$E(D) = 36\Gamma kT\mathrm{e}^{-D/R_F} \quad (1)$$

where $\Gamma = 1/s^2$ is the number density of DNA molecules per unit area (and so the parameter s approximates the mean separation between adjacent strands) and R_F is the Flory radius of the unstructured, single-stranded DNA. Given the geometry of the surfaces in the SFA, eq 1 can be rewritten based on the Derjaguin approximation:[36]

$$\frac{F(D)}{R} = 2\pi E(D) = 72\pi\Gamma kT e^{-D/R_F} \quad (2)$$

Fitting the force profile of the lower-density single-stranded DNA to this equation, we obtain s_{low} = 6.9 nm and R_F = 1.5 nm (Figure 4c), implying that the distance between the molecules on the surface is greater than the diameter of their coiled ensemble and thus, as expected, there is little interaction between adjacent molecules. Instead, the molecules interact only with the surface, which perturbs their otherwise random-flight conformation to produce a mushroom-shaped ensemble.[35]

For the case of higher-density packing we find that our observed force profiles are better described by a brush-regime model. Under these conditions, for which $s < R_F$ and neighboring molecules interact strongly, the interaction potential is approximately exponential[35,36]

$$\frac{F(D)}{R} = 2\pi E(D) = 64\pi\Gamma^{3/2} LkT e^{-\pi D/L} \quad (3)$$

where L is the thickness of the brush layer (Figure 4c). Applying this relationship to the force profiles obtained at higher density gives s_{high} = 0.9 nm and L = 7.1 nm. Under these conditions the distance between adjacent molecules is thus shorter than their Flory radius, which is expected to push them into the brush regime.[5,30] This said, the observed distance, s_{high} = 0.9 nm, is significantly shorter than the ~3 nm mean separation expected at this density, perhaps due to the relatively low precision of our estimates of DNA packing density. In contrast, the thickness of the brush layer is as expected, somewhat shorter than the ~12 nm contour length of a 25-base single-stranded DNA.[33,34]

The distance dependences of the force profiles of surface-attached double-stranded DNA molecules differ from those of single-stranded DNA. At lower density (i.e., single-stranded DNA deposited at ~0.01 chain/nm^2 hybridized to its full length complement at 1 nM) the hard wall repulsion shifts from 2 to 6 nm upon hybridization (Figure 5a). In contrast, at higher density (i.e., ~0.1 chain/nm^2) the hard-wall distance does not measurably change upon hybridization (Figure 5b). We presume this occurs because steric repulsion between neighboring single-stranded molecules in the densely packed submonolayer layer causes them to enter a brush-like regime[9–11] in which they extend to near their full length, as also occurs when they hybridize to form a relatively rigid double helix.

DISCUSSION

We have explored the extent to which the interaction forces and mechanical properties of short surface-tethered DNA molecules are determined by their hybridization state and the density with which they are packed onto the surface. The force–distance profiles we have measured confirm, for example, prior arguments that[10,11] at low densities surface-attached single-stranded DNA submonolayers populate a mushroom-like ensemble. These transition into a brush-like ensemble of thickness approaching their length as the density with which the molecules are packed onto the surface increases. After hybridization, the

double-stranded DNA becomes rod-like,[37] resulting in a stiffer monolayer characterized by longer-range repulsions.

Our findings are consistent with, but significantly extend, the nanomechanical cantilever studies of Wu et al.[22] and theoretical studies by Hagen and Chakraborty.[10] Granick and co-workers found that repulsion starts at distances greater than the contour length expected for single-stranded DNA, an effect they attribute to hydration forces.[20] Similar long-range repulsion was also observed by our SFA work.

Our findings are also consistent with prior AFM-based studies, which have described the height of short, surface-attached DNAs as a function of force at the single molecular level.[38–40] This said, our SFA results provide ensemble-averaged, angstrom-resolved force profiles, rendering it possible to quantitatively characterize the ensemble-driven mushroom-to-brush transition as well as important differences between the properties of single-stranded and double-stranded submonolayers. In doing so, our studies not only confirm previous spectroscopic findings showing that surface-attached single-stranded DNA behaves as a random coil[41,42] but also highlight the structural transition that the DNA undergoes as the areal number density with which it is packed increases, illustrating quantitatively the extent to which it follows polymer scaling theory.[26] Together these results prove quantitative guidelines for the design of biosensors and other technologies reliant on the properties of surface-attached oligonucleotides.

EXPERIMENTAL SECTION

Reagents.

Phosphate buffer (Sigma-Aldrich), sodium chloride (Sigma-Aldrich), 6-mercapto-1-hexanol (Sigma-Aldrich), and tris(2-carboxyethyl)phosphine hydrochloride (Molecular Probes, Carlsbad, CA) were all used as received. The probe and complement DNA sequences were synthesized commercially and used as employed (Biosearch Technologies, Novato, CA). The sequences we employed are as follows:

- Probe: 5′-HS-$(CH_2)_6$-TTATTGATCGGCGTTTTAAAGAAG-3′
- Target: 3′-CTAGCCGCAAAAT-5′
- Probe: 5′-HS-$(CH_2)_6$-ACCCTGAAGTTCATCTGCACCACCG-3′
- Target: 3′-TGGGACTTCAAGTAGACGTGGTGGC-5′

Preparation of the Gold Surface.

Atomically smooth gold surfaces were prepared by using a mica templating technique.[43] A gold layer (45 nm) was deposited on a freshly cleaved mica sheet, which was then glued onto a cylindrical glass disk by using UV-curable glue with the gold layer facing toward the glue. Following curing of the glue (by exposure to UV light for 3 h), the mica sheet was peeled off in ethanol to reveal an atomically smooth gold surface.

DNA Surface Attachment.

DNA-modified surfaces were prepared by using established procedures.[24,44,45] In brief, prior to attachment, the thiol-modified DNA (used as received) was reduced for 1 h at room temperature in the dark in 10 mM tris(2-carboxyethyl)phosphine hydrochloride and then diluted to a final working concentration. To make lower-density submonolayers, the gold surfaces were incubated at room temperature in the dark for 30 min by using a DNA solution diluted to 100 nM in a 10 mM phosphate buffer with 100 mM NaCl, followed by rinsing with deionized water. To make higher density DNA submonolayers, the surfaces were incubated instead at 1 μM DNA solution prepared with a buffer containing 10 mM phosphate and 1 M NaCl for 6 h. Then the surfaces were immersed in 3 mM 6-mercapto-1-hexanol solution for 2 h to "backfill" form the self-assembled monolayer. Following this, the surfaces were rinsed with water and stored in 10 mM phosphate buffer with 100 mM NaCl until use.

Surface Forces Measurements.

We measured the interaction forces between a DNA-modified gold and a bare mica surface with an SFA 2000 and an SFA Mark III (SurForce LLC, Santa Barbara, CA). The detailed experimental setup and force-measuring protocols have been described previously.[46,47] Briefly, a DNA-modified gold surface was mounted in the SFA chamber facing a bare mica surface in a crossed-cylinder geometry (with cylinder radii $R = 2$ cm) as illustrated in Figure 1a; the interaction geometry is locally equivalent to a sphere of radius R against a flat surface when the separation, D, is much smaller than R. Buffer solution was injected between the opposing surfaces and the force, $F(D)$, was then measured as a function of their separation distance (Figure 1a) through the so-called multiple-beam interferometry technique by using "fringes of equal chromatic order" technique with a resolution of ~1 Å. In this work, the reference distance $D = 0$ was determined to be the bare gold–mica contact in air.[46] After completion of the force measurements of the single-stranded DNA monolayer, the sample surface was removed from the SFA chamber and dipped in 15 mL of complementary DNA for 2 h. The surface was then rinsed with 10 mM phosphate buffer, pH 7, with 100 mM NaCl buffer and remounted in the SFA chamber for further subsequent measurements (Figure 1b,c). It is difficult to abolish thermal drift in such experiments, which causes slow, continuous motion of <0.1 Å/s under otherwise static measurement conditions (i.e., after 2 h equilibration in a ±0.1 °C enclosure). We take this drift into account when analyzing our force profiles by fitting it to a small, constant velocity. When we calculate the force profile for approaching, we add this constant velocity, and when analyzing the force of separation, we subtract it.[47,48]

Supplementary Material

Refer to Web version on PubMed Central for supplementary material.

ACKNOWLEDGMENTS

The authors thank Prof. Philip Pincus for helpful discussions.

Funding

This work was supported by the NIH through Grant 1R01GM118560 (K.W.P.), the U.S. Department of Energy, Office of Science, Program in Basic Energy Sciences, Division of Materials Science and Engineering (M.T.), and the Natural Sciences and Engineering Research Council of Canada (NSERC) (H.Z). J.Y. thanks a start-up grant of NTU, M4082049.070.

ABBREVIATIONS

SFA	surface forces apparatus
E-DNA	electrochemical DNA
EAB	electrochemical aptamer-based
SAM	self-assembled monolayer

REFERENCES

(1). Drummond TG; Hill MG; Barton JK Electrochemical DNA sensors. Nat. Biotechnol 2003, 21, 1192–1199. [PubMed: 14520405]

(2). Lubin AA; Plaxco KW Folding-based electrochemical biosensors: the case for responsive nucleic acid architectures. Acc. Chem. Res 2010, 43, 496–505. [PubMed: 20201486]

(3). Hsieh K; Ferguson BS; Eisenstein M; Plaxco KW; Soh H Integrated electrochemical microsystems for genetic detection of pathogens at the point of care. Acc. Chem. Res 2015, 48, 911–920. [PubMed: 25785632]

(4). Kelley SO Advancing Ultrasensitive Molecular and Cellular Analysis Methods to Speed and Simplify the Diagnosis of Disease. Acc. Chem. Res 2017, 50, 503–507. [PubMed: 28945395]

(5). Karzbrun E; Tayar AM; Noireaux V; Bar-Ziv RH Programmable on-chip DNA compartments as artificial cells. Science 2014, 345, 829–832. [PubMed: 25124443]

(6). Tayar AM; Karzbrun E; Noireaux V; Bar-Ziv RH Propagating gene expression fronts in a one-dimensional coupled system of artificial cells. Nat. Phys 2015, 11, 1037–1041.

(7). Halperin A; Buhot A; Zhulina EB Brush effects on DNA chips: thermodynamics, kinetics, and design guidelines. Biophys. J 2005, 89, 796–811. [PubMed: 15908581]

(8). Levicky R; Herne TM; Tarlov MJ; Satija SK Using self-assembly to control the structure of DNA monolayers on gold: A neutron reflectivity study. J. Am. Chem. Soc 1998, 120, 9787–9792.

(9). Opdahl A; Petrovykh DY; Kimura-Suda H; Tarlov MJ; Whitman LJ Independent control of grafting density and conformation of single-stranded DNA brushes. Proc. Natl. Acad. Sci. U. S. A 2007, 104, 9–14. [PubMed: 17190807]

(10). Hagan MF; Majumdar A; Chakraborty AK Nano-mechanical Forces Generated by Surface Grafted DNA. J. Phys. Chem. B 2002, 106, 10163–10173.

(11). Rao AN; Grainger DW Biophysical properties of nucleic acids at surfaces relevant to microarray performance. Biomater. Sci 2014, 2, 436–471. [PubMed: 24765522]

(12). Kegler K; Konieczny M; Dominguez-Espinosa G; Gutsche C; Salomo M; Kremer F; Likos CN Polyelectrolyte-Compression Forces between Spherical DNA Brushes. Phys. Rev. Lett 2008, 100, 118302–118304. [PubMed: 18517835]

(13). Li D; Banon S; Biswal SL Bending dynamics of DNA-linked colloidal particle chains. Soft Matter 2010, 6, 4197–4204.

(14). Bracha D; Karzbrun E; Shemer G; Pincus PA; Bar-Ziv RH Entropy-driven collective interactions in DNA brushes on a biochip. Proc. Natl. Acad. Sci. U. S. A 2013, 110, 4534–4538. [PubMed: 23471983]

(15). Shon MJ; Rah S; Yoon T Submicrometer elasticity of double-stranded DNA revealed by precision force-extension measurements with magnetic tweezers. Sci. Adv 2019, 5, No. eaav1697. [PubMed: 31206015]

(16). Yu J; Zhou J; Sutherland A; Wei W; Shin YS; Xue M; Heath JR Microfluidics-based single-cell functional proteomics for fundamental and applied biomedical applications. Annu. Rev. Anal. Chem 2014, 7, 275–295.

(17). Rant U; Arinaga K; Fujita S; Yokoyama N; Abstreiter G; Tornow M Dynamic Electrical Switching of DNA Layers on a Metal Surface. Nano Lett. 2004, 4, 2441–2445.

(18). Peterson AW; Wolf LK; Georgiadis RM Hybridization of mismatched or partially matched DNA at surfaces. J. Am. Chem. Soc 2002, 124, 14601–14607. [PubMed: 12465970]

(19). Nelson BP; Grimsrud TE; Liles MR; Goodman RM; Corn RM Surface plasmon resonance imaging measurements of DNA and RNA hybridization adsorption onto DNA microarrays. Anal. Chem 2001, 73, 1–7. [PubMed: 11195491]

(20). Cho YK; Kim S; Lim G; Granick S A Surface Forces Study of DNA Hybridization. Langmuir 2001, 17, 7732–7734.

(21). Gong P; Harbers GM; Grainger DW Multi-technique comparison of immobilized and hybridized oligonucleotide surface density on commercial amine-reactive microarray slides. Anal. Chem 2006, 78, 2342–2351. [PubMed: 16579618]

(22). Wu G; Ji H; Hansen K; Thundat T; Datar R; Cote R; Hagan M; Chakraborty A; Majumdar A Origin of nanomechanical cantilever motion generated from biomolecular interactions. Proc. Natl. Acad. Sci. U. S. A 2001, 98, 1560–1564. [PubMed: 11171990]

(23). Pawlak R; Vilhena JG; Hinaut A; Meier T; Glatzel T; Baratoff A; Gnecco E; Pérez R; Meyer E Conformations and cryo-force spectroscopy of spray-deposited single-strand DNA on gold. Nat. Commun 2019, 10, 685. [PubMed: 30737410]

(24). Ricci F; Lai RY; Plaxco KW Linear, redox modified DNA probes as electrochemical DNA sensors. Chem. Commun 2007, 36, 3768–3770.

(25). White RJ; Phares N; Lubin AA; Xiao Y; Plaxco KW Optimization of Electrochemical Aptamer-Based Sensors via Optimization of Probe Packing Density and Surface Chemistry. Langmuir 2008, 24, 10513–10518. [PubMed: 18690727]

(26). de Gennes PG Conformations of Polymers Attached to an Interface. Macromolecules 1980, 13, 1069–1075.

(27). Murphy MC; Rasnik I; Cheng W; Lohman TM; Ha T Probing single-stranded DNA conformational flexibility using fluorescence spectroscopy. Biophys. J 2004, 86, 2530–2537. [PubMed: 15041689]

(28). Anderson TH; Donaldson SH; Zeng H; Israelachvili JN Direct Measurement of Double-Layer, van der Waals, and Polymer Depletion Attraction Forces between Supported Cationic Bilayers. Langmuir 2010, 26, 14458–14465. [PubMed: 20735021]

(29). Smith SB; Finzi L; Bustamante C Direct mechanical measurements of the elasticity of single DNA molecules by using magnetic beads. Science 1992, 258, 1122–1126. [PubMed: 1439819]

(30). Zuker M Mfold web server for nucleic acid folding and hybridization prediction. Nucleic Acids Res. 2003, 31, 3406–3415. [PubMed: 12824337]

(31). Fernández de Ávila BE; Watkins HM; Pingarrón JM; Plaxco KW; Palleschi G; Ricci F Determinants of the Detection Limit and Specificity of Surface-Based Biosensors. Anal. Chem 2013, 85, 6593–6597. [PubMed: 23713910]

(32). Peterson AW; Heaton RJ; Georgiadis RM The effect of surface probe density on DNA hybridization. Nucleic Acids Res. 2001, 29, 5163–5168. [PubMed: 11812850]

(33). Bockelmann U; Essevaz-Roulet B; Heslot F DNA strand separation studied by single molecule force measurement. Phys. Rev. E: Stat. Phys., Plasmas, Fluids, Relat. Interdiscip. Top 1998, 58, 2386–2394.

(34). Chi Q; Wang G; Jiang J The persistence length and length per base of single-stranded DNA obtained from fluorescence correlation spectroscopy measurements using mean field theory. Phys. A 2013, 392, 1072–1079.

(35). Israelachvili JN Intermolecular and Surface Forces, 3rd ed.; Academic Press: Burlington, MA, 2011.

(36). Leckband D; Israelachvili JN Intermolecular forces in biology. Q. Rev. Biophys 2001, 34, 105–267. [PubMed: 11771120]

(37). Mackor EL The Growth of Uniform Colloidal Dispersions. J. Colloid Sci 1951, 6, 492.

(38). Wang K; Goyer C; Anne A; Demaille C Exploring the Motional Dynamics of End-Grafted DNA Oligonucleotides by in Situ Electrochemical Atomic Force Microscopy. J. Phys. Chem. B 2007, 111, 6051–6058. [PubMed: 17487999]

(39). Husale S; Persson HHJ; Sahin O DNA nanomechanics allows direct digital detection of complementary DNA and microRNA targets. Nature 2009, 462, 1075–1078. [PubMed: 20010806]

(40). Bosco A; Bano F; Parisse P; Casalis L; DeSimone A; Micheletti C Hybridization in nanostructured DNA monolayers probed by AFM: theory versus experiment. Nanoscale 2012, 4, 1734–1741. [PubMed: 22301788]

(41). Kimura-Suda H; Petrovykh DY; Tarlov MJ; Whitman LJ Base-dependent competitive adsorption of single-stranded DNA on gold. J. Am. Chem. Soc 2003, 125, 9014–9015. [PubMed: 15369348]

(42). Petrovykh DY; Perez-Dieste V; Opdahl A; Kimura-Suda H; Sullivan JM; Tarlov MJ; Himpsel FJ; Whitman LJ Nucleobase orientation and ordering in films of single-stranded DNA on gold. J. Am. Chem. Soc 2006, 128, 2–3. [PubMed: 16390092]

(43). Chai L; Klein J Large Area, Molecularly Smooth (0.2 nm rms) Gold Films for Surface Forces and Other Studies. Langmuir 2007, 23, 7777–7783. [PubMed: 17559240]

(44). Xiao Y; Lai RY; Plaxco KW Preparation of electrode-immobilized, redox-modified oligonucleotides for electrochemical DNA and aptamer-based sensing. Nat. Protoc 2007, 2, 2875–2880. [PubMed: 18007622]

(45). Kang D; Ricci F; White RJ; Plaxco KW Survey of Redox-Active Moieties for Application in Multiplexed Electrochemical Biosensors. Anal. Chem 2016, 88, 10452–10458. [PubMed: 27659949]

(46). Yu J; Kan Y; Rapp M; Danner E; Wei W; Das S; Miller DR; Chen Y; Waite JH; Israelachvili JN Adaptive hydrophobic and hydrophilic interactions of mussel foot proteins with organic thin films. Proc. Natl. Acad. Sci. U. S. A 2013, 110, 15680–15685. [PubMed: 24014592]

(47). Israelachvili JN; Min Y; Akbulut M; Alig A; Carver G; Greene W; Kristiansen K; Meyer E; Pesika N; Rosenberg K; Zeng H Recent advances in the surface forces apparatus (SFA) technique. Rep. Prog. Phys 2010, 73, 036601.

(48). Beyder A; Spagnoli C; Sachs F Reducing probe dependent drift in atomic force microscope with symmetrically supported torsion levers. Rev. Sci. Instrum 2006, 77, 056105.

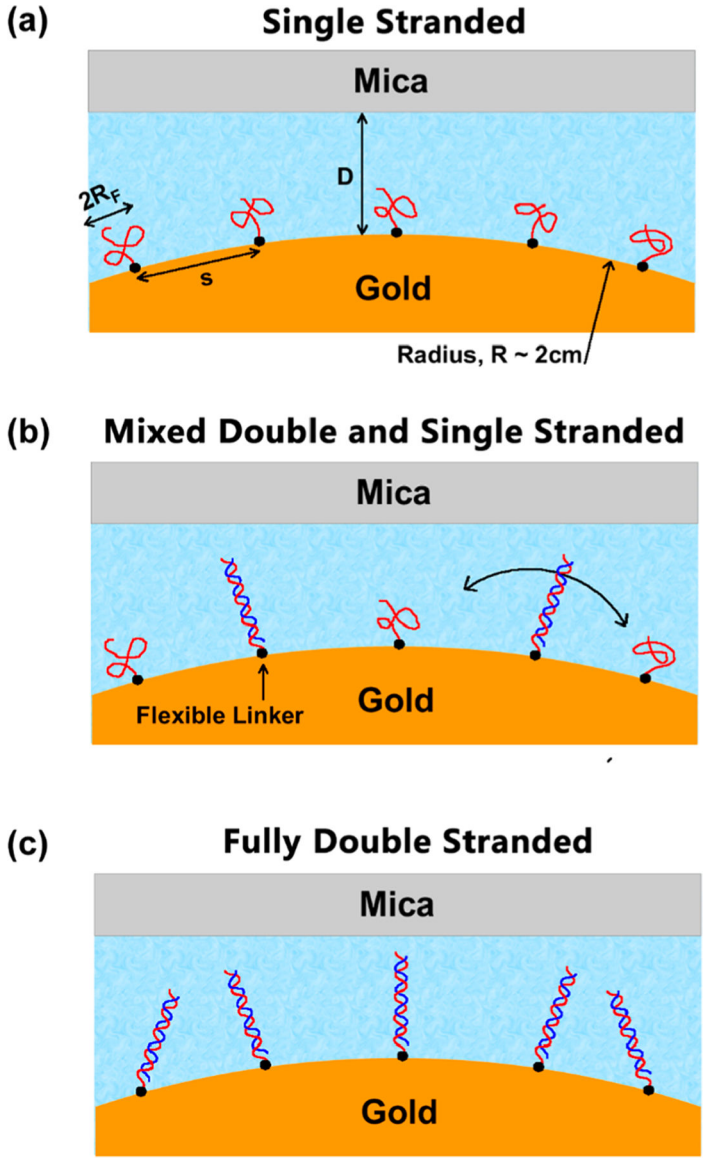

Figure 1.

Using a surfaces forces apparatus (SFA), we have measured the interactions between a gold surface modified with a submonolayer of DNA in a variety of hybridization states and a bare mica surface as a function of the distance between the opposing surfaces. The surfaces include those modified with (a) single-stranded DNA (R_F is the Flory radius, s is the distance between the attachment sites of adjacent molecules), (b) surfaces upon which some of the DNA molecules are hybridized to full-length or partial-length complementary strands and some DNA molecules remain single-stranded, and (c) surfaces for which every DNA molecule is in its fully (or partially) hybridized, double-helical state. In these experiments, the separation between the two surfaces can be varied in both directions.

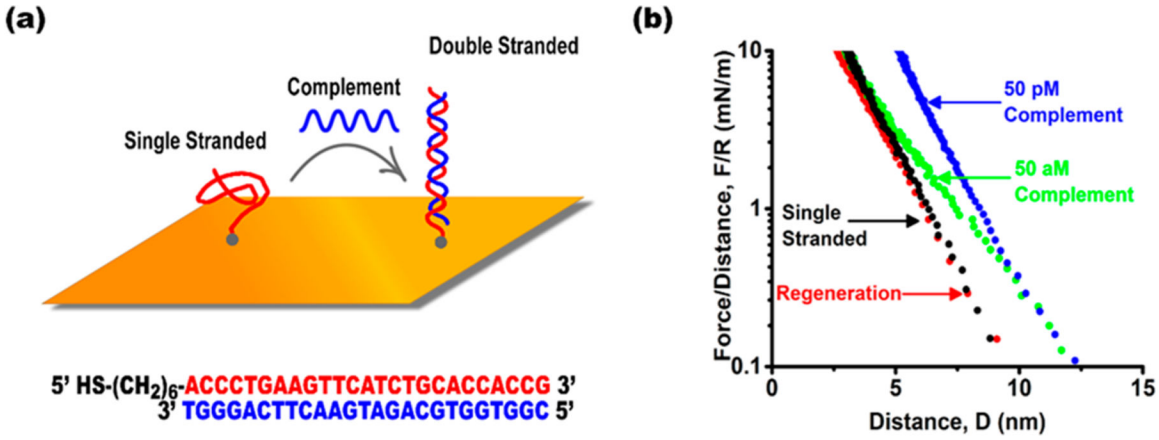

Figure 2.

(a) Hybridization alters the structure, interactions, and mechanical properties of a surface modified via the terminal attachment of a submonolayer of a 25-base DNA. (b) During the transition from all DNA in its single-stranded for (black curve) to effectively all DNA in its double-stranded form (blue curve), the range at which repulsion is first detected shifts from 10 to 15 nm. At intermediate levels of hybridization (i.e., approximately equal numbers of single-stranded and double-stranded molecules; green curve) we observe intermediate behavior. After "regeneration" (i.e., regeneration of the single-stranded form via a wash at low ionic strength) we observe a force profile (red curve) effectively identical with that first measured for the single-stranded form.

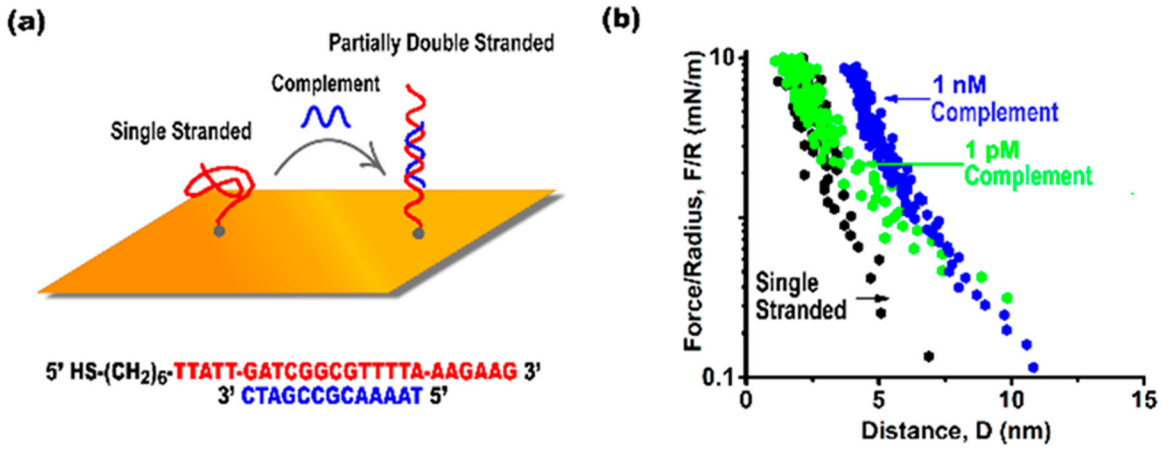

Figure 3.

(a) We have also investigated the effects of creating a partially double-stranded DNA on the surface by challenging the 25-base, single-stranded construct with a 13-base sequence complementary to its middle, leaving six bases of single-stranded DNA on either end of the double helix. (b) Here, too, force profiles shift to longer ranges upon hybridization, albeit less than is seen with the full-length double-stranded construct (Figure 2).

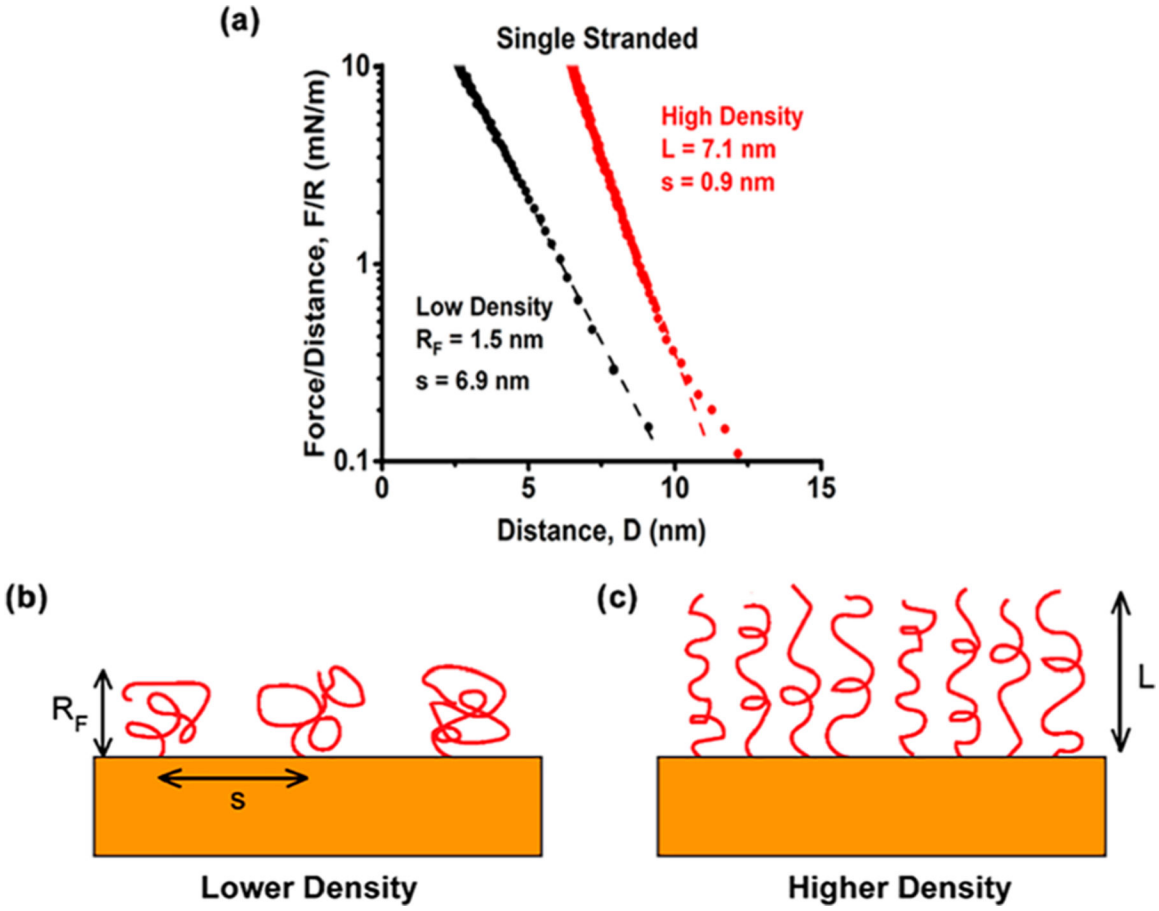

Figure 4.

Increasing the areal number density, Γ, with which a single-stranded DNA is packed onto the surface changes the mechanical properties of the DNA submonolayer. (a) At a lower density (Γ ~ 0.01 chain/nm^2), for example, the force profile is largely monophasic (i.e., fits to a single line on a semilog plot), and the repulsion force is first observed at 10 nm. Fitting this force profile by using a "mushroom" polymer model (panel b) gives a coil radius, R_F, of 1.5 nm and a mean separation, s_{low}, of 6.9 nm. These values are consistent with both the estimated density with which DNAs are packed onto the surface (which corresponds to a mean separation of ~10 nm). They are also consistent with theoretical predictions that mushroom behavior will be observed when $s > R_F$. In contrast, the force profile is clearly biphasic (exhibits two distinct log–linear regimes differing in slope) at higher densities (Γ ~ 0.1 chain/nm^2), and the detectable repulsion begins at a separation of 16 nm. Fitting this force profile with a "brush model" (panel c) gives a brush thickness, L, of 7.1 nm and s_{high} of 0.9 nm.

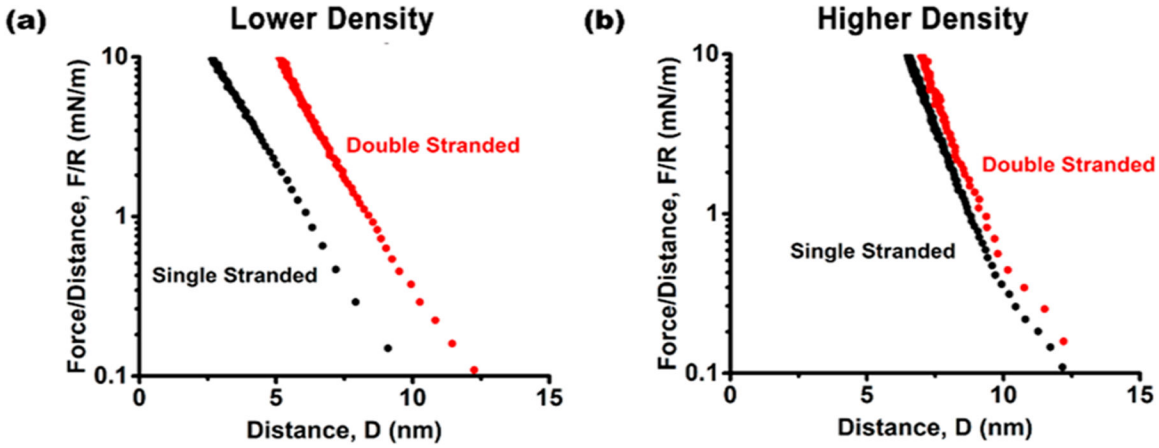

Figure 5.

(a) At lower density (Γ ~ 0.01 chain/nm^2), hybridization shifts the force profile ~4 nm toward longer distances. (b) At higher density (Γ ~ 0.1 chain/nm^2), in contrast, hybridization does not significantly alter the force profile, presumably because the polymer brush formed under high-packing-density conditions extends the single-stranded DNA molecules in a manner similar to that seen upon hybridization.